JOURNAL OF MATERIALS SCIENCE 37 (2002) 2103–2107

Effect of Ni on the wear behavior of a zinc-aluminum alloy

P. CHOUDHURY, S. DAS, B. K. DATTA
Department of Metallurgical and Materials Engineering, Indian Institute of Technology, Kharagpur-721302, India
E-mail: sdas@metal.iitkgp.ernet.in

In this investigation, an attempt has been made to examine the effect of Ni on the wear response of a high-aluminum zinc alloy. The alloy has been modified with 0.3 and 0.9 wt% Ni, and wear tests have been carried out at sliding speeds of 3.925 and 6.54 m/s. The wear characteristics have been correlated with their microstructural features. The unmodified alloy exhibits inferior wear behavior with the increase in sliding speed. The improved wear response of the modified alloys is due to the presence of Ni_3Al phase formed throughout the matrix. Moreover, the improvement of the modified alloy is more significant at the higher speed of sliding and also with the increase in Ni content. This study indicates that it is possible to develop modified versions of high-aluminum zinc-based alloys having much improved wear characteristics; the information gains special attention in view of the high speed of sliding used in this study.

1. Introduction

Zinc-aluminum (ZA) alloys, with a unique combination of properties, have been found to be alternative materials to most aluminum casting alloys, bearing bronzes, cast iron, plastics, and steel fabrications. These alloys feature clean, low-temperature, energy-saving melting, excellent castability, high strength, and equivalent or often superior bearing properties as compared to standard bronze bearings [1].

However, the major problems suffered by these alloys are property deterioration at high temperatures (above 100–120°C) and dimensional instability with rising temperature [2–5]. The dimensional instability is caused by the rapid decomposition of the Al-solid solution into a Zn-base solid-solution and $CuZn_4$ phases after aging [5].

In order to overcome the problem of dimensional instability, earlier attempts have been made to partially replace copper by some high-melting element like Ni and Si [2–4]. The earlier investigators studied the effect of composition modification, i.e., the addition of Ni + Si, on the dry sliding wear behavior of the zinc-aluminum alloy. An attempt has been made to explain the wear behavior on the basis of the microstructural features of the alloys [2–4].

The present study investigates the abrasive wear behavior of zinc-aluminum alloys containing moderate and high amount of Ni along with a reduced amount of copper. The investigation has been carried out at two different speeds but under a constant load.

Abrasive wear is caused by the sliding action of hard particles on a softer solid surface resulting in the displacement or detachment of the material. The mechanisms of wear depend on physical and chemical interactions between different elements of the tribosystem, resulting in the detachment of material from the solid surface [6]. Compared to unlubricated sliding wear, the value of the wear coefficient can be much greater in abrasive or erosive wear [7–11]. Adhesion, abrasion, deformation, heating, surface fatigue, and fracture are the events occurring during the interaction between hard particles and a solid surface.

Several material properties like hardness, elastic modulus, yield strength, melting temperature, crystal structure, microstructure, and composition have been shown to have some effect on abrasive wear [12].

2. Experimental

2.1. Alloy preparation

Alloys were prepared by conventional melting and casting route in the form of 16 mm square cross-section, 160 mm long castings. Casting was done in cast-iron moulds. The chemical compositions of the alloys are given in Table I.

2.2. Microscopy & X-Ray diffraction (XRD) study

Microstructural characterization of the alloys was carried out on samples similar to those used for wear testing. The specimens were metallographically polished according to standard practices and etched suitably. Diluted nitric acid (5 vol%) in water was used as the etchant. Wear surfaces were examined using a JEOL scanning electron microscope (SEM) attached with an energy dispersive x-ray spectroscopic (EDS) facility.

X-ray diffraction study has been carried out at 40 kV and 20 mA operating conditions and at a scanning rate of 1°/min. Cobalt target ($\lambda = 1.79$A) and nickel filter have been used.

TABLE I Chemical compositions of the experimental alloys

Alloy designation	Elements (wt%)				
	Al	Cu	Mg	Ni	Zn
ZA1	30.4	1.80	0.04	–	Balance
ZNi1	26.2	1.56	0.04	0.265	Balance
ZNi3	25.95	1.58	0.04	0.884	Balance

2.3. Hardness

Bulk hardness of all the alloys were measured using a Brinell hardness tester, with a 10 mm-diameter steel-ball indenter and under a load of 500 kg. The application time of the load was 60 seconds.

2.4. Wear behavior

Abrasive wear tests were carried out on 16 mm square cross-section samples having thickness of 7 mm, against 320 grit SiC paper affixed to a rotating flat disc of 250 mm diameter [13]. The speeds selected for the study were 300 rpm (3.925 m/s) and 500 rpm (6.54 m/s). All the experiments were carried out under a constant load of 10.9 N. The tests were conducted for a total time of 300 seconds, which corresponds to sliding distances of 1177.5 m and 1962.5 m for the speeds of 300 and 500 rpm, respectively.

Wear rates of the specimens were computed by the weight loss technique. A Sartorius make electronic balance was used for weighting the specimens. Prior to weighing, the specimens were cleaned with ethanol to remove the wear debris. Wear data have been plotted as weight loss per unit applied load per unit area of specimen surface as a function of time (seconds).

3. Results

3.1. Microstructure & X-Ray diffraction (XRD) study

Fig. 1 shows the microstructural features of the alloys. Alloy ZA1 (refer Table I) revealed the presence of primary α dendrites, surrounded by the $\alpha + \eta$ eutectoid product in the interdendritic regions (Fig. 1a), regions marked A and B, respectively). The features of ZNi1 and ZNi3 are similar to those of ZA1, except for the additional Ni containing phases (Fig. 1b and c, region marked C). The EDS analysis combined with XRD results suggests that the intermetallic phase (particle C of Fig. 1b or c) formed is Ni_3Al.

The powder x-ray diffraction pattern obtained from alloy ZNi3 is shown in Fig. 2. It is evident from this figure that Ni_3Al is the only Ni-Al intermetallic phase formed in this alloy.

3.2. Hardness

The results of the bulk hardness measurement are given in Table II.

TABLE II Bulk hardness of the experimental alloys

Alloy designation	Bulk hardness HB 10/500/60
ZA1	119
ZNi1	124
ZNi3	130

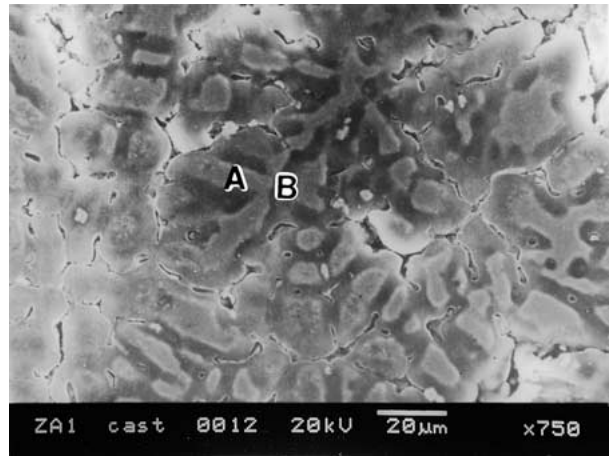

(a)

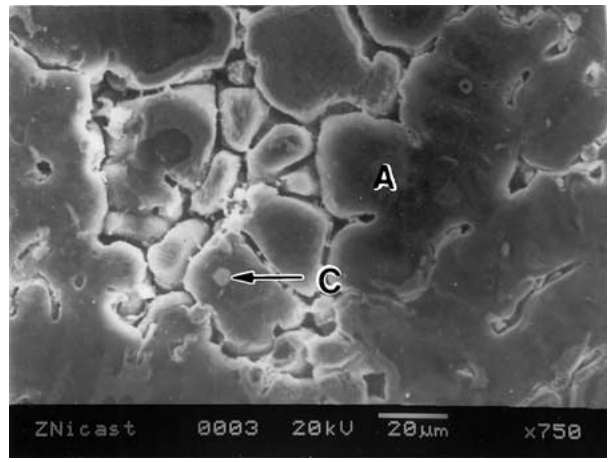

(b)

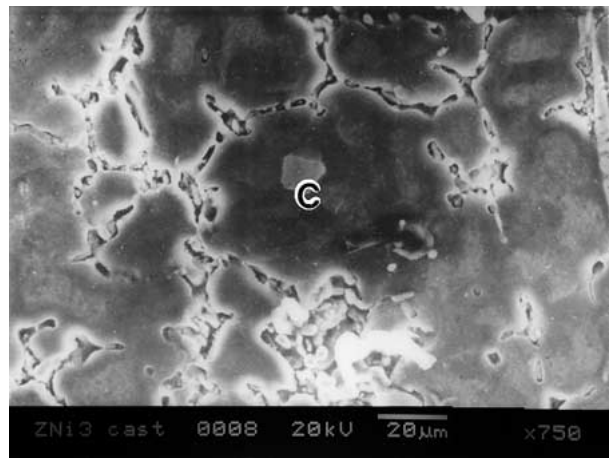

(c)

Figure 1 SEM micrographs (secondary electron) of the as-cast alloys (a) SEM micrograph of ZA1; (b) SEM micrograph of ZNi1; (c) SEM micrograph of ZNi3.

3.3. Wear behavior

The wear behavior of the alloys is plotted as a function of time in Figs 3 and 4. The wear rate initially increases with time. However, after some time the wear curves tend to taper off showing a parabolic wear behavior. ZA1 shows the maximum wear resistance at 300 rpm, but undergoes the maximum wear at 500 rpm. This alloy undergoes 33.75% increase in wear loss (after 300 seconds of wear) with the increase in speed from 300 to 500 rpm. After 300 seconds of wear, ZNi1 undergoes 7.55% decrease in wear loss as the test speed

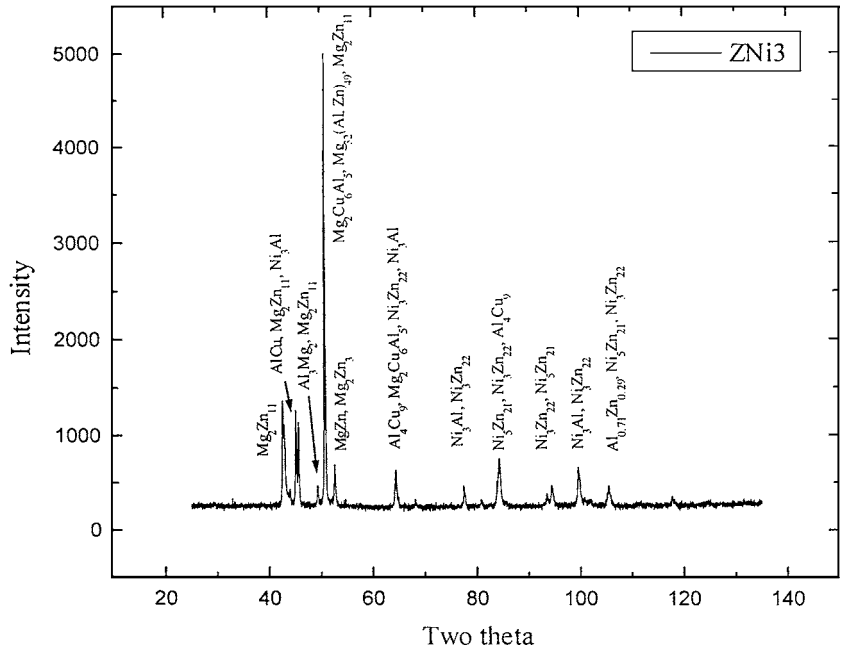

Figure 2 X-Ray diffraction pattern of ZNi3.

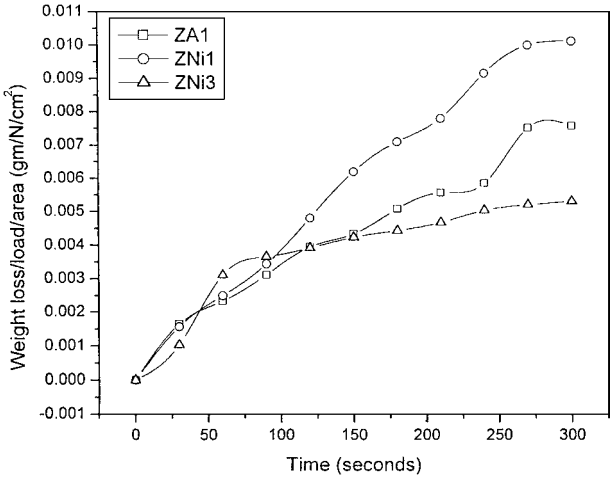

Figure 3 Wear loss as a function of time at 300 rpm.

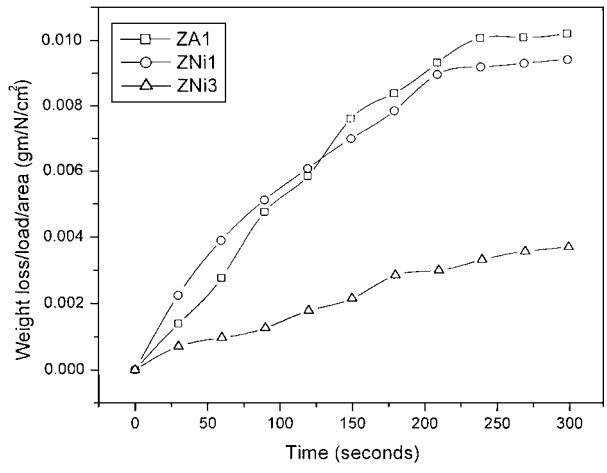

Figure 4 Wear loss as a function of time at 500 rpm.

increases from 300 to 500 rpm. With the increase in Ni, there is further decrease in wear loss. This is revealed in the case of ZNi3, which undergoes 30.79% decrease in wear loss (after 300 seconds of abrasion) as the speed increases to 500 rpm.

3.4. Wear surfaces

Wear surfaces of ZA1 are shown in Fig. 5. A relatively clean surface marked by shallow scratches, as shown in Fig. 5a, indicates the low wear loss undergone by ZA1 at 300 rpm. A surface marked by deep scratches along with grooves, as shown in Fig. 5b, indicates that wear is caused predominantly by plowing mechanism.

Wear surfaces of ZNi1 are shown in Fig. 6. The high wear loss at 300 rpm, shown in Fig. 6a, is indicated by extensive and deep grooves. Surface cracks are also observed. Plowing mechanism is possibly the main mode of wear.

Fig. 7 shows the wear surfaces of ZNi3. Low wear loss at 300 rpm is indicated by the presence of shallow scratches, shown in Fig. 7a. At 500 rpm, wear loss is still low as evident from the surface shown in Fig. 7b.

4. Discussion

The zinc-aluminum alloys (Table I) fall in the hypereutectoid range considering the zinc-aluminum equilibrium diagram [14]. The phase to form first is the primary α (the solid-solution of zinc in aluminum). In the process, the excess Zn is rejected to the surrounding liquid, which finally transforms to eutectoid $\alpha + \eta$. Accordingly, ZA1 comprises of primary α dendrites surrounded by the eutectoid $\alpha + \eta$ (Fig. 1a, regions marked A and B, respectively). The presence of Ni in the alloys ZNi1 and ZNi3 has led to the formation of the intermetallic phase, Ni_3Al (Fig. 1b and c, region marked C). The dendritic regions (Fig. 1a–c, regions marked A), have Al rich composition. The interdendritic regions also show high Al content (as observed in the EDS results), which is probably due to overlapping signals from the surrounding Al rich dendrites. The interdendritic regions have a high concentration of Cu and Ni. The Ni_3Al phases formed in ZNi1 and ZNi3 are very hard (Knoop micro-indentation hardness $\sim$242 kg/mm^2 [15]). However, owing to the higher aluminum content of ZA1 (Table I), the effect of Ni on the

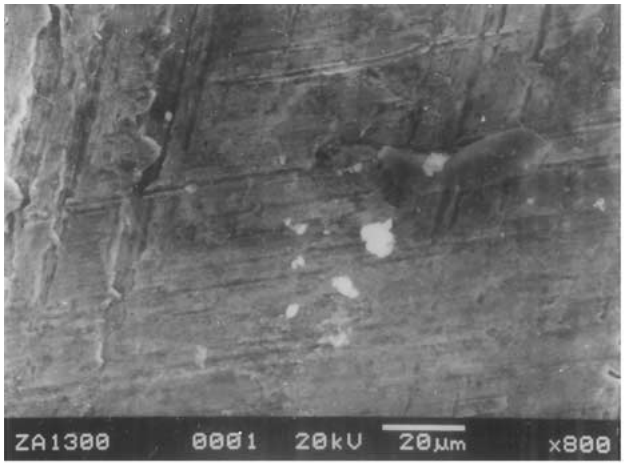

(a)

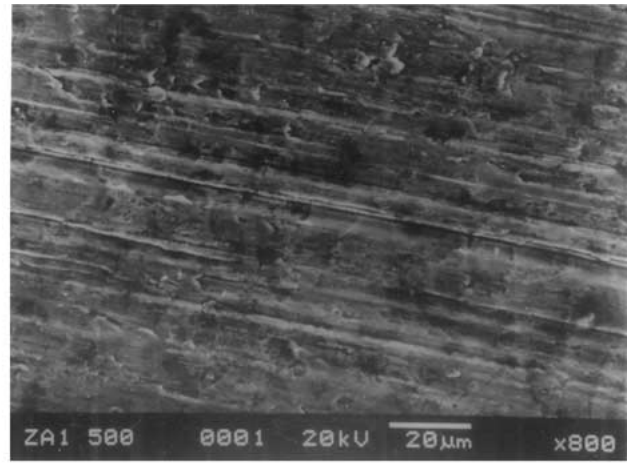

(b)

Figure 5 SEM micrographs (SE) of worn surfaces of ZAl at (a) 300 rpm and (b) 500 rpm.

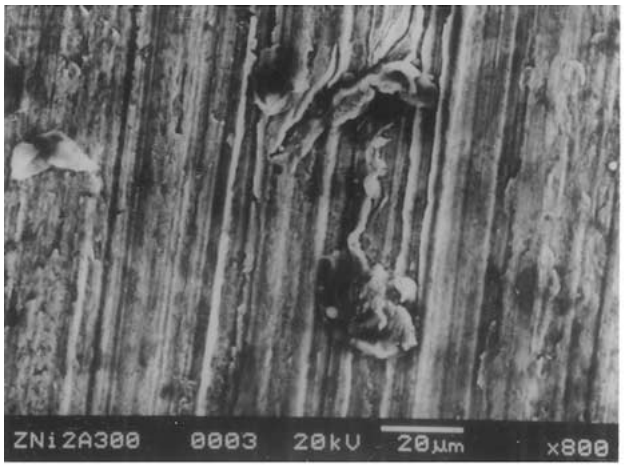

(a)

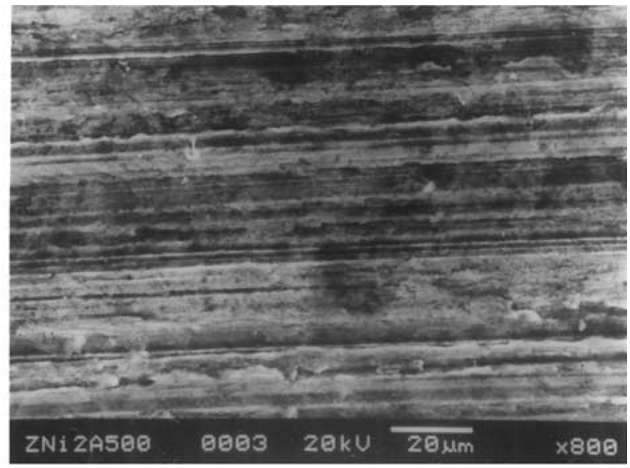

(b)

Figure 6 SEM micrographs (SE) of worn surfaces of ZNi1 at (a) 300 rpm and (b) 500 rpm.

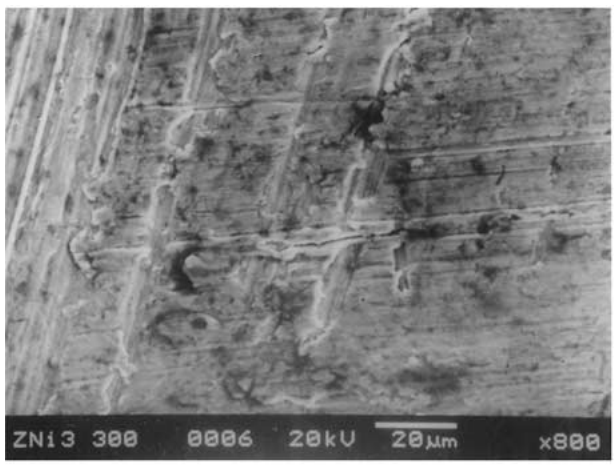

(a)

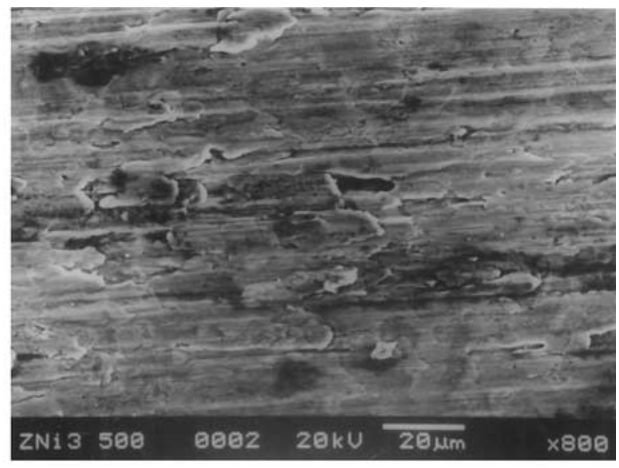

(b)

Figure 7 SEM micrographs (SE) of worn surfaces of ZNi3 at (a) 300 rpm and (b) 500 rpm.

bulk hardness of ZNi1 and ZNi3 is not very significant (Table II).

The modified alloys have a fairly uniform distribution of the Ni_3Al particles. The presence of Ni_3Al is also evident from the x-ray diffraction pattern in Fig. 2. Ni_3Al peaks are observed at $\theta = 22.7137$, 32.1747, 38.8653 and 49.9474 degrees.

During abrasion the temperature of the contact surface is much higher than the bulk, more so at the higher speed of testing. Moreover, the temperature at the point

of contact of the intermetallic phase and the SiC particles is even higher than the rest of the contact surface.

Experimentally, the temperature of the bulk sample during abrasion has been determined by means of an infrared pyrometer. Using the standard heat flow equation, the temperature at the contact point of the Ni_3Al and SiC particles has been roughly estimated to be in the range of 550–600°C. The calculations are based on the assumption that heat conduction is one directional, and that half the surface area is being abraded by the SiC particles.

It is known that Ni_3Al exhibits anomalous yield behavior, i.e., the yield strength increases with the rise in temperature reaching a maximum in the range of 400–650°C and then falling [16]. Since the estimated temperature stated above falls in this range, it can be inferred that the high yield strength of the Ni_3Al particles during abrasion is responsible for the low wear loss of ZNi3. This is particularly significant at 500 rpm where the temperature rise is even higher.

ZNi1, having a lower amount of Ni and hence lesser fraction of Ni_3Al, does not exhibit a pronounced similar behavior as ZNi3. The higher wear loss suffered by ZNi1 at 300 rpm is possibly due to micro-cracking at the Ni_3Al/matrix interface. At .500 rpm, the rise in temperature results in a plastic flow of the soft zinc matrix, which aids in welding up of the micro-cracks.

It is known that ZA alloys suffer from deterioration of properties with the rise in temperature [2–5]. Hence, ZA1, the unmodified alloy, suffers from higher wear loss with the increase in speed, and therefore with the increase in temperature.

5. Conclusions

(a) The addition of Ni, even in small amount (0.3 to 0.9 wt%), to the zinc-aluminum alloy results in the formation of Ni-containing intermetallic phases (e.g., Ni_3Al, Ni_3Zn_{22} and Ni_5Zn_{21}).

(b) Ni_3Al is the only nickel-aluminide (Ni-Al intermetallic phase) formed in the modified alloys.

(c) An addition of Ni in appropriate amount reduces the abrasion wear loss of a high-aluminum zinc alloy.

(d) The reduction in wear loss owing to the addition of Ni is more pronounced at the higher speed of testing.

(e) Improvement in wear resistance increases with the amount of Ni.

(f) The anomalous yield behavior of Ni_3Al, formed in the modified alloys, results in an improvement of wear behavior at higher speed and hence higher temperature.

References

1. E. J. KUBEL JR., *Adv. Mater. Proc.* **132** (1987) 51.
2. B. K. PRASAD, A. K. PATWARDHAN and A. H. YEGNESWARAN, *Met. & Mat. Trans.* A **27A** (1996) 3513.
3. T. CALAYAG and D. FERREA, *Soc. of Automotive Engineers* **90** (1982) 40.
4. B. K. PRASAD, A. K. PATWARDHAN and A. H. YEGNESWARAN, *Scripta Mat.* **37** (1997) 323.
5. Y. CHEN and M. TU, *Mat. Sci. & Tech.* **14** (1998) 473.
6. K. H. ZUM GAHR, *Tribology Intl.* **31** (1998) 587.
7. J. T. BURWELL and C. D. STRANG, *Proc. R. Soc.* A **212** (1952) 470.
8. J. F. ARCHARD, *J. Appl. Phys.* **24** (1953) 981.
9. E. RABINOWICZ, in "Friction & Wear of Materials" (John Wiley, New York, 1965).
10. I. M. HUTCHINGS, in "Tribology: Friction & Wear of Engg. Materials" (Edward Arnold, London, 1992).
11. K. HOKKIRIGAWA, in Proceedings of Surface Modification Technology VIII, edited by T. S. Sudarshan and M. Jeandin (Inst. of Materials, London, 1995) p. 93.
12. J. H. TYLCZAK and A. OREGON, "ASM Handbook," Vol. 18, 8th ed. (American Society for Metals, Metals Park, Ohio, 1973) p. 186.
13. P. P. BANDOPADHYAY, S. DAS, S. MADHUSUDAN and A. B. CHATTOPADHYAY, *J. Mater. Sci. Lett.* **18** (1999) 727.
14. J. L. MURRAY, "Binary Alloy Phase Diagrams," Vol. 1, 2nd ed. (ASM International, Materials Park, Ohio, 1990) p. 239.
15. P. J. BLAU, "ASM Handbook," Vol. 18, 8th ed. (American Society for Metals, Metals Park, Ohio, 1973) p. 774.
16. M. YAMAGUCHI and Y. UMAKOSHI, *Prog. In Mat. Sci.* **34** (1990) 37.

Received 3 November 2000
and accepted 24 January 2002